ANTICANCER RESEARCH *34*: 49-60 (2014)

Tumor-specific Localization of Self-assembled Nanoparticle PET/MR Modalities

ISTVÁN HAJDU[1,2,3], GYÖRGY TRENCSÉNYI[4], MAGDOLNA BODNÁR[1], MIKLÓS EMRI[4], GÁSPÁR BÁNFALVI[5], JUDIT SIKULA[2], TERÉZ MÁRIÁN[4], JÓZSEF KOLLÁR[2], GYÖRGY VÁMOSI[3] and JÁNOS BORBÉLY[1,2]

[1]*BBS Nanotechnology, Debrecen, Hungary;*
Departments of [2]*Radiology,* [3]*Biophysics and Cell Biology and*
[4]*Nuclear Medicine, Medical and Health Science Center, University of Debrecen, Debrecen, Hungary;*
[5]*Department of Microbial Biotechnology, Faculty of Science and Technology, University of Debrecen, Debrecen, Hungary*

Abstract. *Aim: The aim of this work was to synthesize and study in vitro and in vivo nanocarriers used as magnetic resonance imaging (MRI) contrast agents that accumulate in tumor cells specifically overexpressing folate receptors. Materials and methods: Nanoparticles were prepared by self-assembly of poly-γ-glutamic acid and chitosan biopolymers and were complexed with gadolinium ions. Folic acid served as a targeting molecule. Rat hepatocellular carcinoma (HeDe) cells overexpressing folate receptors were used as a model system. For in vivo experiments, HeDe cells were transplanted under the renal capsule of F344 rats. Results: In vitro results showed the significant internalization of nanoparticles into HeDe cells. MRI measurements revealed that targeting nanocarriers accumulated in tumors. The MRI/PET fusion images resulted in the exact localization of tumors. Conclusion: The nanocarrier provides a suitable means for the early diagnosis of tumors based on their overexpression of folate receptors.*

The potential utility of nanosystems as improved contrast agents for medical imaging has generated a great deal of scientific activity in recent years. Nanosystems have the potential to improve medical imaging by increasing the specificity and sensitivity of images and to allow for the combination of images from multiple modalities, increasing the probability of earlier disease diagnosis and more effective intervention. Several different contrast agents are currently used to enhance sensitivity and to provide high resolution soft-tissue contrast for magnetic resonance imaging (MRI). The paramagnetic gadolinium-containing contrast agents shorten the relaxation time of protons in water to provide higher contrast at tumor sites relative to the surrounding tissues based on the differing densities of tumor *vs*. healthy tissues.

Targeted delivery is an emerging platform in nano-medicine, therefore many studies have focused on the development of efficient targeted delivery systems. A useful strategy to achieve efficient tumor targeting is to conjugate carriers with specific ligands that recognize and bind to their cognate receptors on the surface of cancer cells. Targeting ligands shown to be effective in pre-clinical and early clinical studies include monoclonal antibodies (1, 2), peptides (3-5), transferrin (6-8), somatostatin (9-10), aptamers (11, 12) and folic acid (FA) (13-15).

Recent studies have indicated that FA receptors are selectively overexpressed in a number of tumor cell types (*e.g.* breast, ovarian, cervical, colorectal, renal, and nasopharyngeal), but present in low or non-detectable levels in most normal cells. FA has a low molecular weight, high receptor affinity (16), and is internalized *via* receptor-mediated endocytosis (17, 18), making it a good targeting candidate for nanocarriers delivering a contrast agent to the cell's interior.

Numerous publications attest to the efficacy of FA-targeted nanoparticles. Nanocarriers including micelles (19, 20), dendrimers (21, 22), liposomes (23, 24), metallic nanoparticles (25, 26), and polymeric nanoparticles (27, 28) have been shown to be targeted to cancer cells by FA.

Correspondence to: György Vámosi, Department of Biophysics and Cell Biology, Medical and Health Science Center, University of Debrecen, Egyetem tér 1 H-4032 Debrecen, Hungary. Tel/Fax: +36 52412623 e-mail: vamosig@med.unideb.hu and János Borbély, BBS Nanotechnology, H-4225 Debrecen 16, Hungary. Tel/Fax: +36 52541742 e-mail: janos.borbely@bbsnanotech.eu

Key Words: MRI, PET, contrast agent, gadolinium, *in vitro*, *in vivo*, self-assembled nanoparticles.

Molecular imaging plays a very important role in molecular diagnosis. Molecular imaging enables visualization of the targeted biological tissues and an understanding of its complexities for diagnosis of the disease. Real-time imaging of targeted tissues provides a profound understanding of fundamental biological processes and helps diagnose various diseases (29). Given the strengths and weakness of specific imaging modalities, it is difficult to obtain all the necessary information about the biological structure and function of an organ using any single one, therefore attempts are being made to fuse the advantages of different imaging techniques by combining two or more imaging modalities (30, 31).

The fusion of MRI and PET images has proven to be beneficial as it provides images of high sensitivity and high resolution.

In cancer staging, integrated whole-body PET-MRI provides a metabolic and anatomic image at the same time. Thus, *in vivo* clinical studies may benefit from the advantages of both modalities, such as high sensitivity of positron emission tomography (PET) and the best resolution of MRI. Another benefit compared to widely used PET-CT (computed tomography) is that the MRI modality has no radiation component. Progress in technological development of PET detector technology and MRI-based PET attenuation correction. To provide a new generation of contrast agents for hybrid machines, two-in-one nanoparticulate systems are in development for dual-modality use (32-34).

In our recent study, biodegradable poly-γ-glutamic acid and biocompatible chitosan biopolymers were combined to produce stable, self-assembled nanoparticles. The factors determining the physicochemical properties of the nanoparticles have been described previously (35). *In vitro* cytotoxicity and *in vivo* toxicity studies demonstrated the preferential uptake of FA-coupled nanoparticles by cancer cells (36).

The present investigation reports the synthesis and the application of a biodegradable, macromolecular, folate-targeted MRI contrast agent tested against the *in vitro* and *in vivo* growth of hepatocellular carcinoma (*HeDe*) tumor cell line. *HeDe* is a chemically-induced animal tumor cell line which overexpresses extracellular FA receptor (37, 38).

In this study, *in vitro* results confirm that the nanocarriers are internalized into the targeted *HeDe* tumor cells in a folate receptor-dependent manner. For *in vivo* experiments, tumor cells were transplanted under the renal capsule of F344 rats. Using this method abdominal tumors and metastasis were modeled.

MRI results support the conclusion that the targeted nanocarriers accumulate in the tumor and change its relaxation time. After *i.v.* ^{18}F-FDG administration, tumor localization was performed using our mini-PET method (see Materials and Methods), and by fusing MRI-PET images both anatomical and functional aspects were gained. This combined method allows for identification of tumor localization unequivocally, enabling early tumor diagnosis.

Materials and Methods

Materials. Chitosan [CH; degree of deacetylation (DD)=88%, Mv=320 kDa] was purchased from Sigma-Aldrich Co., Budapest, Hungary. Chitosan was dissolved in 2.0% aqueous acetic acid solution to give a polymer concentration of 1.0% (w/w), and then filtered and dialyzed against distilled water until the pH of the water outside the dialysis tubing became neutral. The product was dried by lyophilization to obtain a white chitosan powder and used for further experiments. Poly-γ-glutamic acid (γ-PGA; Mw=400 kDa) was purchased from the Vedan Group, Taiwan. For purification, γ-PGA was dissolved in water to give a polymer concentration of 1.0% (w/w), dialyzed against distilled water, and freeze-dried to obtain purified γ-PGA for further experiments. Water-soluble 1-[3-(dimethylamino)propyl]-3-ethylcarbodiimide methiodide (EDC), FA dehydrate and gadolinium(III)-chloride ($GdCl_3$) hydrate were purchased from Sigma-Aldrich Co., and were used without further purification. The sodium salt of Alexa Fluor® 488 succinimidyl ester fluorescent dye was purchased from Molecular Probes Eugene, OR, USA.

Synthesis of folated γ-PGA. FA was conjugated *via* the amino groups to γ-PGA using the EDC technique: γ-PGA aqueous solution (V=100 ml, 0.5 mg/ml, pH=6.5), was prepared, and EDC (10 mg in distilled water) was added dropwise. The reaction mixture was stirred at 4˚C for 1 h, then at room temperature for 1 h. FA (18 mg dissolved in 4 ml dimethyl sulfoxide) was then added to the reaction mixture and stirred at room temperature for 24 h. The folated poly-γ-glutamic acid (γ-PGA-FA) was purified by dialysis against distilled water for five days.

Synthesis of fluorescently labeled chitosan. Aqueous solution of chitosan was mixed with Alexa Fluor® 488 dye. Briefly, chitosan was dissolved in 0.1 M hydrochloric acid, and then adjusted to pH 6.5 with 0.1 M sodium hydroxide solution. To 2 ml of chitosan solution (1 mg/ml), 5 μl of Alexa Fluor® 488 dye (9.1 mg/ml) was mixed and the reaction mixture was stirred at room temperature for 24 h. Fluorescently-labeled chitosan (CH-AF) was purified by dialysis against distilled water for five days.

Preparation of self-assembled nanoparticle gadolinium conjugate. Stable self-assembled nanoparticles were prepared *via* an ionotropic gelation process between the folated γ-PGA and fluorescently-labeled chitosan linear chains. CH-AF solution was added into the γ-PGA-FA solution under constant stirring. An opaque aqueous colloidal system containing nanoparticles that remained stable at room temperature for several weeks at physiological pH was achieved. To produce paramagnetic contrast agent, the self-assembled nanoparticles were conjugated with Gd^{3+}. The solution of GdCl3 was added dropwise to the aqueous colloid system containing targeted self-assembled nanoparticles and stirred at room temperature for 30 min. The schematic view of the self-assembled nanoparticle-gadolinium complex (γ-PGA-FA/CH-AF–Gd) is shown in Figure 1.

Non-targeted nanoparticles complexed with Gd-ions were also prepared by self-assembly of folate-free γ-PGA and fluorescently labeled chitosan as a control for *in vitro* studies.

Characterization of nanoparticles. The hydrodynamic size of particles was measured by dynamic light scattering (DLS) using a Zetasizer Nano ZS (Malvern Instruments Ltd., Grovewood, Worcestershire, UK). This system is equipped with a 4 mW helium/neon laser with a wavelength of 633 nm and measures particle size with noninvasive backscattering technology at a detection angle of 173˚. Measurements were performed using a particle-sizing cell in automatic mode. The mean hydrodynamic diameter was calculated from the autocorrelation function of the intensity of light scattered from the particles. Electrokinetic mobility of the nanoparticles was determined in a folded capillary cell (Malvern) with a Zetasizer Nano ZS apparatus. Transmittance of the nanoparticle solution was measured with a Hitachi U-1900 spectrophotometer (Hitachi High-Technologies Corporation. Tokyo, Japan) at an operating wavelength of λ=500 nm in optically homogeneous quartz cuvettes. Measurements were repeated three times, and their average value was calculated. The morphological characterization of nanoparticles in dried state was carried out with a Hitachi 3000N scanning electron microscope (Hitachi Science Systems Ltd., Japan) (SEM).

Cell culture. Hepatocellular carcinoma (*HeDe*) cell line (38) was cultured as an exponentially-growing monolayer in RPMI 1640 supplemented with 10% fetal bovine serum (FBS), 100 U/ml penicillin and 100 μg/ml streptomycin (37˚C, 5% CO_2), passaged daily. Cell viability was more than 95%, as assessed by trypan blue dye exclusion.

MTT assay. The toxicity of the γ-PGA-FA/CH-AF-Gd nanoparticles on hepatocarcinoma cells (HeDe) was investigated using MTT assay. *HeDe* cells (1.5×10^3) were seeded in 96-well plates (BD Falcon, Germany) and incubated overnight. Cells incubated with cell growth medium (RPMI 1640) served as negative controls. γ-PGA-FA/CH-AF-Gd nanoparticles were diluted in *HeDe* cell growth medium to 30 μg nanoparticles/ml then 100 μl cell growth medium and nanoparticle-containing medium was added to each well. Cells were incubated for 24 h. After the incubation, the medium was removed and 10 μl MTT (3-(4,5-dimethylthiazol-2-yl)-2,5-diphenyltetrazolium bromide) (5 mg/ml) was added. After 3 h incubation, 100 μl dimethyl sulfoxide was added to each well. The optical density of wells were measured with a microplate reader at λ=492 nm.

Confocal microscopy of cellular uptake of nanoparticles. Equal number of *HeDe* cells (2×10^4 per well) were plated in an 8-well cell culture chamber. Ten microliters of nanoparticle – gadolinium conjugate was added to the cells at a concentration of 0.3 mg/ml per well and cells were then incubated at 37˚C for 24 h in RPMI medium. The medium was removed by aspiration and wells were washed consecutively with 400 μl of cold phosphate buffered saline (PBS), citrate buffer solution and PBS. The fixation was performed with 300 μl/well of fresh 1% formaldehyde in PBS at 4˚C for 10 min. Samples were imaged by an Olympus FluorView 1000 confocal microscope (Olympus, Tokyo, Japan) using a ×60 UPLSAPO oil immersion objective. Excitation of Alexa Fluor® was performed at 488 nm wavelength by an Ar ion laser and detection of images at 500-550 nm. Images were analyzed using the Olympus FluoView FV10-ASW 1.5 software package (Olympus, Tokyo, Japan).

Pre-treatment of HeDe cells with free FA. To test whether nanoparticle uptake occurs *via* folate receptors, 4 μl FA (11 mg/ml in dimethyl sulfoxide) was added to the tumor cells to saturate receptors. Cells were incubated with free FA at 37˚C for 1 h, and then treated with nanoparticles.

Flow cytometry. *HeDe* cells were plated at a density of 1 million cells per T flask (75 cm^2), and then incubated in a 5% (v/v) CO_2 humidified atmosphere at 37˚C for 24 h in RPMI. After culturing cells to sub-confluency (80-90%), 1 ml of γ-PGA-FA/CH-AF–Gd contrast agent (0.3 mg/ml) was added to each T flask and cells were incubated at 37˚C for an additional 24 h. After the incubation, the medium was removed and cells were washed, trypsinized (0.25% trypsin/0.05% EDTA) and centrifuged. The cell pellet was dissolved in fresh 2% formaldehyde in PBS.

Flow cytometric analysis (BD FACSArray Bioanalyzer System, BD Biosciences, Franklin Lakes, NJ, USA) was carried out with a single-cell suspension, and only the live cells were gated based on forward and side scatter dot plots. Data are given as the mean channel fluorescence of the cell population.

Magnetic resonance imaging in vitro. *HeDe* cells (2×10^6 in 15 ml RPMI-1640) were incubated with folate-targeted γ-PGA-FA/CH-AF–Gd and non-folated γ-PGA/CH-AF–Gd nanoparticles. Nanoparticles (1.5 ml) at a concentration of 0.3 mg/ml were added to the cells and incubated at 37˚C for 24 h in RPMI-1640 medium. After the incubation, the medium was removed and cells were washed with PBS and trypsinized using 2 ml of trypsin/EDTA (0.25%/0.05%) and centrifuged. The cell pellet obtained was re-suspended in 200 μl sterile PBS. Vials containing cell suspensions were kept in a container filled with distilled water during the measurement. T1-Weighted signal intensities were measured by a clinical 1.5 T GE Signa LX MR scanner (GE Healthcare Waukesha, WI, USA). The pulse sequences were TR=420.0 ms and TE=20.0 ms; thickness: 1.5 mm and space: 0 during the measurements.

Recipient animal model. In each experiment, adult male Fischer 344 (F344) rats (Charles River Mo Kft., Gödöllő, Hungary), weighting 150-200 g, were used (n=10). Rats were kept in a conventional laboratory environment and fed a semi-synthetic diet (Charles River Mo, Kft, Godollo, Hungary) and tap water *ad libitum*. Animals received human care to the criteria outlined in the "Guide for the Care and Use of Laboratory Animals" (39) authorized by the Ethical Committee for Animal Research, University of Debrecen, Hungary (permission number: 22/2007).

Experimental tumor. We used the hepatocellular carcinoma (Hepatocarcinoma Debreceniensis, *HeDe*) isolated from Fischer 344 rats which were treated at newborn age by injecting *i.p.* 125 μg/animal N-nitroso-dimethylamine (Sigma-Aldrich Kft, Budapest, Hungary) in saline. Tumors were removed 5-7 months after chemical tumorogenesis, minced into smaller pieces and tumor slices were frozen and the *HeDe* cell line was established (37, 40).

Experimental surgery. For transplantation 10^6 cells (*HeDe* cell line) in 10 μl saline were placed on Gelaspon^R disc (Germed, Rudolstadt, Germany). Experimental animals were anesthesized by intraperitoneal administration of 6 mg/100 g body weight pentobarbital (Nembutal, CevaPhylaxia Rt. Budapest, Hungary). The retroperitoneum was opened by abdominal section, the left kidney was exposed and the tumor cell containing gelatin disc was placed under the renal capsule (40). Stitches were put in the wound and *in vivo* experiments followed 10 days later.

Magnetic resonance imaging in vivo. For MRI imaging, tumor-bearing rats (n=5) were injected with targeted nanoparticle-gadolinium complex as an MRI contrast agent *via* the tail vein 24 h before the MRI investigation, at the dosage of 17.3 μmol Gd/kg. After this incubation time, the rats were anaesthetized with pentobarbital (Nembutal; 6 mg/100 g body weight). T1-Weighted MR images were performed using a clinical 1.5 T GE Signa LX MR scanner. The pulse sequences were TR=420.0 ms and TE=20.0 ms; thickness: 1.5 mm and space: 0 during the measurements. Comparison of tumor signal intensity between γ-PGA-FA/CH-AF–Gd contrast agent-treated and control groups were calculated using an unpaired Student's *t*-test. All data were tested to be normal distributed by means of Kolmogorov-Smirnov test. Data are reported as the mean±SD and $p \leq 0.05$ was considered statistically significant.

PET imaging in vivo. A small-animal PET scanner (MiniPET-II, Debrecen, Hungary; www.minipetct.hu) was used for *in vivo* imaging. The MiniPET-II small animal PET scanner consists of 12 detector modules in one ring with LYSO scintillator crystal blocks and position-sensitive photomultiplier tubes (Hamamatsu H9500). Each crystal block comprises 35×35 pins of 1.27×1.27×12 mm size (pitch size of 1.35 mm). The sensitivity value in the center of the field of view (FOV) is 6.3 cps/kBq and the system's absolute sensitivity is 11.4% (NEMA-NU4 2008). The axial and the radial FOV are 48 mm and 106 mm, respectively.

For PET imaging, tumor bearing rats were injected 15±2 MBq ^{18}F-FDG *via* the tail vein. One hour after tracer injection rats were anaesthetized with pentobarbital (Nembutal; 6 mg/100 g body weight) and static PET data were acquired for 10 min at each bed position (five bed positions/rat). The collected data were subjected to a rebinning algorithm and an ML-EM iterative method to reconstruct the images (voxel size: 1.34×0.2×0.2 mm^3).

Results

Formation of tumor-targeted nanoscopic MRI contrast agent. Folate-targeted, self-assembled nanoparticles were formed from biopolymers based on an ionotropic gelation process. The nanoparticles can make stable complexes with Gd ions to obtain paramagnetic contrast agent. The physicochemical properties of the γ-PGA-FA/CH-AF–Gd nanoparticular contrast agents were studied.

At a biopolymer concentration of 0.3 mg/ml, the transmittance of nanoparticles was 85%. The aqueous solution of nanoparticles was slightly opalescent and stable for several weeks. The hydrodynamic size of the nanoparticles was 130±4 nm with a relatively narrow size distribution between 70 and 280 nm (Figure 2a) (nanoparticles were suspended in 5% glucose solution, which was also used in the *in vivo* experiments). Dried nanoparticles were visualized by SEM micrograph (Figure 2b), and confirmed to be of an estimated size variation between 50 and 150 nm. The mobility of nanoparticles was μ=–3.8±0.3 μmcm/Vs at pH 7.4.

Cytotoxicity of γ-PGA-FA/CH-AF-Gd. The viability of *HeDe* cells treated with γ-PGA-FA/CH-AF-Gd nanoparticles was investigated using the MTT assay. The MTT assay indicated no significant change in cell viability at 30 μg/ml nanoparticle concentration, which is suited to cell labeling.

Cellular uptake of γ-PGA-FA/CH-AF–Gd contrast agent. Specific cellular uptake of nanoparticles by *HeDe* cancer cells overexpressing folate receptors was tested by using confocal microscopy. Figure 3 shows the confocal microscopic fluorescence images of the *HeDe* cells incubated with targeting (Figure 3a) and non-targeting (Figure 3b) contrast agent. The folated γ-PGA-FA/CH-AF–Gd nanoparticles accumulated in the cancer cells to a significantly greater extent than their non-folated counterparts.

To confirm the receptor specificity of cellular uptake, *HeDe* cells were incubated with free folic acid to block or drastically reduce folate receptors held on the surface of cancer cells prior to treatment with targeting γ-PGA-FA/CH-AF–Gd contrast agent. FA-treated cells serve as a model of healthy cells, which express only a low number of folate receptors. Figure 3c shows that the targeting nanoparticles do not internalize into the model healthy cells compared with the *HeDe* tumor cells overexpressing folate receptors supporting a specific, receptor-dependent uptake mechanism.

Figure 3d shows optical slices of *HeDe* cells treated with folate-targeting γ-PGA-FA/CH-AF–Gd contrast agent. The microscopic images show that targeted nanoparticles entered the cell and were present in the cytoplasm with the notable exception of the round nucleus in the middle of the cell.

Flow cytometric analysis of folate receptor dependent nanoparticle uptake. The tumor cell targeting efficacy of folate-targeted nanoparticulate contrast agent and non-folated nanoparticles was compared using FACS analysis. *HeDe* cells incubated with folate-targeted nanoparticles, a significant shift in fluorescence spectrum was observed relative to the control, non-treated *HeDe* cells while only minor spectral displacement was registered relative to cells incubated with non-folated nanoparticles (Figure 4).

In vitro MR investigation. The T1-weighted MRI of tumor cell suspensions treated with the nanoparticles were recorded to test the efficacy of nanoparticles as a potential MR contrast agent (Figure 5). The control cell suspension (Figure 5a) similarly to the MR images of *HeDe* cells incubated with non-folated γ-PGA/CH-AF–Gd nanoparticles generated low signal intensity due to the low level of internalized nanoparticles (Figure 5b). Folated nanoparticles internalized and accumulated in the targeted tumor cells, which appears as a bright enhancement (Figure 5c). The signal intensities of the control cells and cell suspension incubated with non-folated nanoparticles were similar, 441 and 511 on the densitometer scale, respectively. On the contrary, the signal

intensity value of *HeDe* cell suspension incubated with folated nanoparticles was 869, significantly higher than the previous values, appearing as a bright area.

In vivo MRI investigation. The folate-mediated *in vivo* uptake of γ-PGA-FA/CH-AF–Gd contrast agents was evaluated using Fischer 344 rats bearing *HeDe* tumors (n=10). Animals (n=5) treated with 5% glucose solution served as a control. Tumor-bearing rats were imaged with T_1-weighted MR (Figure 6 a and b). There was a significantly stronger increase in signal intensity in tumors 24 h after intravenous injection of γ-PGA-FA/CH-AF–Gd compared to control. Comparing the signal intensity values significant ($p<0.001$) differences were found between the control and the γ-PGA-FA/CH-AF–Gd-treated tumors. The signal intensities of control and treated tumors were 396.8±7.3 and 595.2±3.4, respectively (Figure 6c).

The anatomy of the rat model is exhibited by MRI (Figure 7a), which reveals the location of the tumor. The PET image (Figure 7b) shows the metabolism, suggesting the existence of the tumor but gives minimal information about its location because the contours of the surrounding organs are not visible as they are in the MRI.

Fusion of MR and PET images (Figure 7c) combine anatomic and metabolic information. Colored parts of the fusion image show the enhanced metabolism of the tumor, while the anatomic picture provided by MRI allows for its accurate localization.

Discussion

Formation of tumor-targeted nanoscopic MRI contrast agent. Nanoparticles were prepared as a contrast agent that would increase the signal of MRI. γ-PGA and chitosan biopolymer formation took place *via* an ionotropic gelation process. Nanoparticles assembled into a stable complex with Gd^{3+} ions, changing the local magnetic field and thereby increasing MR signals and providing a suitable MRI contrast agent. Chitosan was fluorescently-labeled to facilitate the visual observation of the contrast agent by confocal microscopy or detection by flow cytometry. FA as targeting ligand was conjugated to the γ-PGA biopolymer allowing nanoparticles to be internalized by cancer cells overexpressing folate receptors. Conjugates lacking FA served as a control in cellular uptake studies.

Cellular uptake of γ-PGA-FA/CH-AF–Gd contrast agent. Nanoparticles containing FA as targeting ligand bound to *HeDe* cells overexpressing folate receptors and were efficiently internalized (Figure 3a). In contrast, particles lacking FA did not penetrate the cell membrane (Figure 3b), in fact their non-sepcific adsorption to the cell membrane was negligible as well.

To confirm the receptor specificity of cellular uptake, *HeDe* cells were incubated with free FA to block folate receptors held on the surface of cancer cells prior to treatment with targeting γ-PGA-FA/CH-AF–Gd contrast agent. The targeting nanoparticles were not taken up into the model healthy cells (Figure 3c) compared with the *HeDe* tumor cells overexpressing folate receptors, supporting a specific, receptor-dependent uptake mechanism.

Optical slices of *HeDe* cells after treatment with folate-targeting contrast agent (Figure 3d) indicate that our contrast agent developed into folate-targeted nanoparticles was internalized into *HeDe* cells. To the contrary, there was no significant accumulation of the nanoparticles when they lacked folate or when the cell surface was saturated with free FA to mimic healthy cells expressing only few folate receptors. This observation suggests that by using tumor-specific contrast agents, side-effects can be minimized.

Flow cytometric analysis of folate receptor-dependent nanoparticle uptake. FACS analysis of *HeDe* cells (Figure 4) confirmed the specific internalization and accumulation of folated nanoparticles in the targeted tumor cells. In sharp contrast to the folated nanoparticles, the spectral shift of non-folated γ-PGA/CH-AF–Gd nanoparticles was minimal compared to the controls. These results support the folate receptor-specific uptake of nanoparticles. FA as targeting ligand is required for the targeted internalization. The insignificant accumulation of non-folated nanoparticles in tumor cells suggests that their side-effects can be minimized.

In vitro MR investigation. To directly verify that folated nanoparticles targeting *HeDe* cells can be used as MRI contrast agents, studies with an MRI scanner were undertaken. T_1-Weighted MRI were observed to test the efficacy of nanoparticles as a potential MRI contrast agent (Figure 5). The folated nanoparticles internalized and accumulated in the targeted tumor cells (Figure 5c), and their paramagnetic properties caused a reduction in the T_1 relaxation time, thereby changing the signal intensity, appearing as a bright enhancement. The MRI of control cell suspension (Figure 5a) and *HeDe* cells incubated with non-folated nanoparticles (Figure 5b) resulted in a similar darker area with low signal intensity values. The non-folated nanoparticles due to the low level of their internalization do not change the relaxation time and signal intensity of tumor cells. On the contrary, the signal intensity value of *HeDe* cell suspension incubated with folated γ-PGA-FA/CH-AF–Gd nanoparticles was significantly higher due to their effective internalization.

In vivo MRI investigation. Fischer rat models were used for the *in vivo* experiments. *HeDe* cells were transplanted under

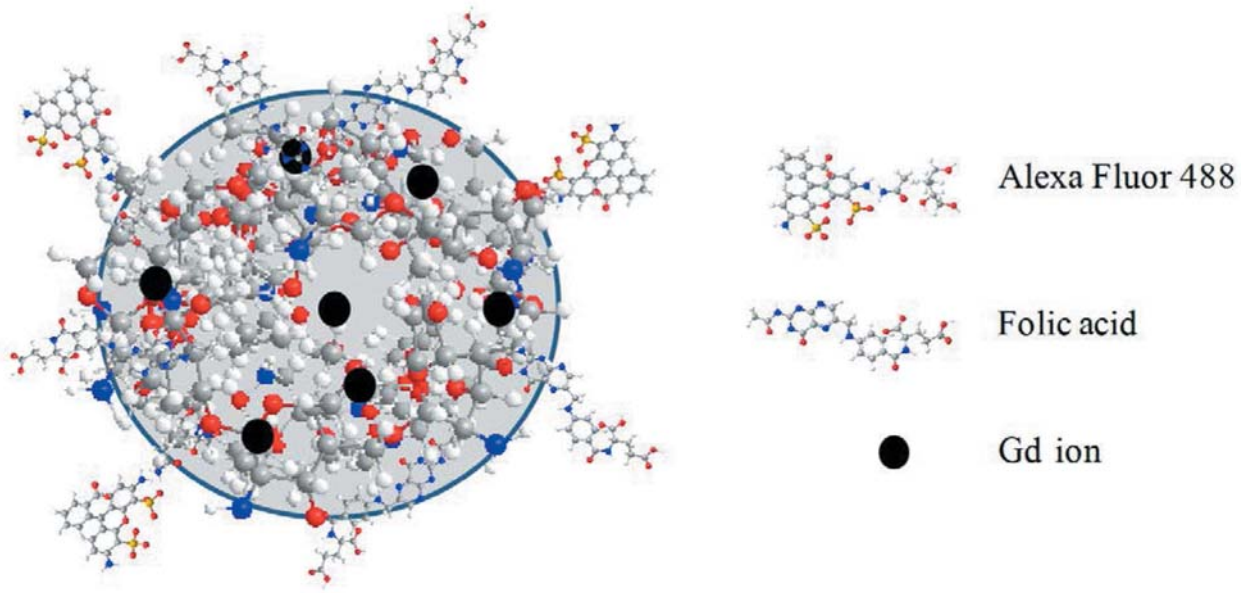

Figure 1. *Schematic representation of the targeted nanocarrier gadolinium complex.*

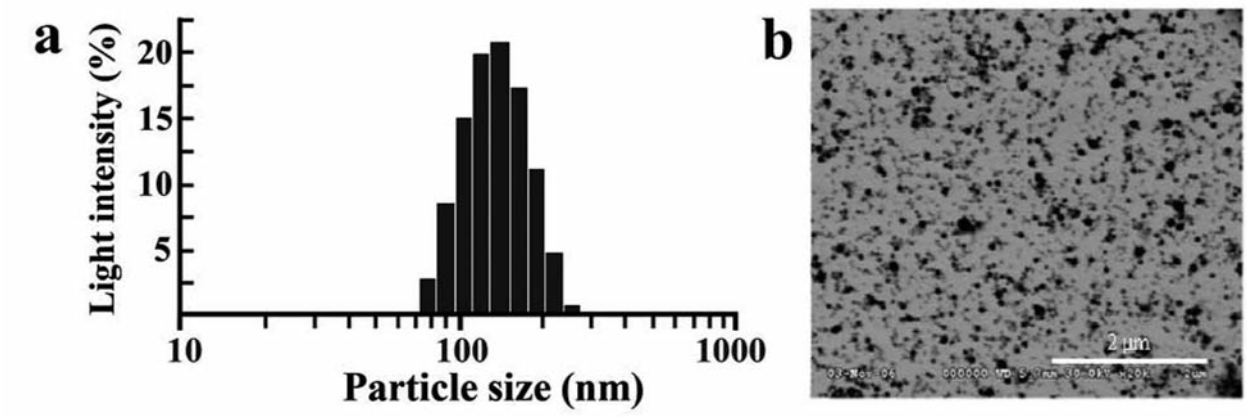

Figure 2. *Hydrodynamic size distribution (a) and SEM micrograph (b) of γ-PGA-FA/CH-AF–Gd contrast agent.*

the renal capsule of left kidney of animals, and the tumor-bearing animal models were imaged 10 days later.

The MRI provides the anatomic image of the animal. The folated, targeting γ-PGA-FA/CH-AF–Gd contrast agent internalized preferentially in tumor cells due to their overexpression of folate receptors. The accumulation of nanoparticles caused signal enhancement due to the presence of the paramagnetic Gd ligand, in steep contrast to the surrounding tissue, aiding in the exact localization of the tumor. These changes in signal intensities can also be clearly seen in the T1-weighted MRI (Figure 6a and b). The high uptake of γ-PGA-FA/CH-AF–Gd by the tumor indicates that the accumulation is related to folate-mediated endocytosis. This finding supports the conclusion that the folate-targeting γ-PGA-FA/CH-AF–Gd contrast agents were internalized preferentially in tumor cells as they are overexpressing folate receptors.

The MRI confirms that the folated nanoparticles accumulate in the targeted tumor cells, and due to the transported paramagnetic ions, change the relaxation time, appearing as a bright contrast. The PET image shows the metabolism and supports the tumor localization.

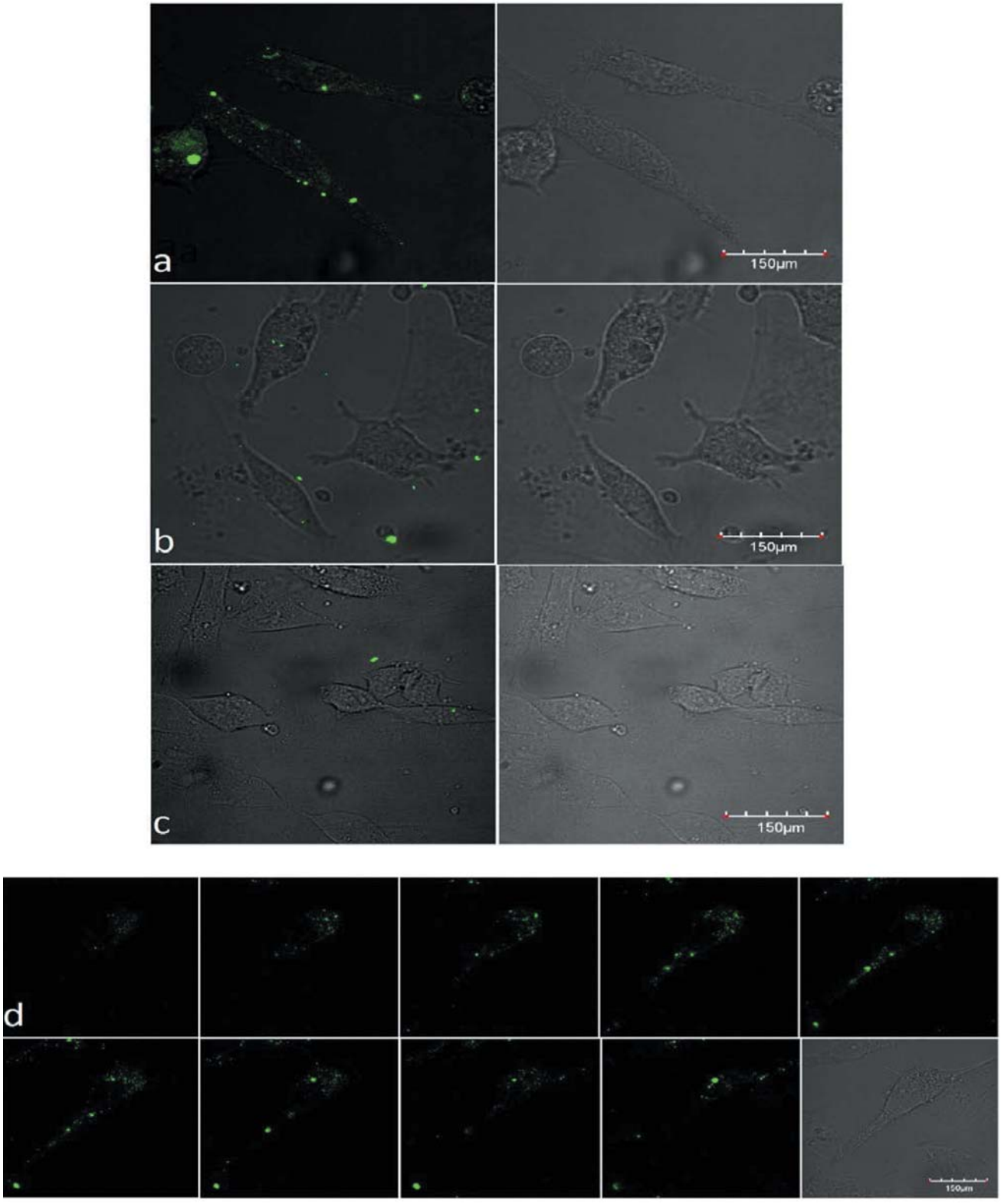

Figure 3. *Confocal microscopic images of HeDe cells treated with folate-targeting γ-PGA-FA/CH-AF–Gd (a), non-folated γ-PGA/CH-AF–Gd (b), and folate-targeting γ-PGA-FA/CH-AF–Gd after incubating cells with free folic acid (c); and confocal microscopic sections of a HeDe cancer cells incubated with γ-PGA-FA/CH-AF–Gd nanoparticles (z-series: 1.5 µm/slice thickness; from the bottom of the cell to the top) (d).*

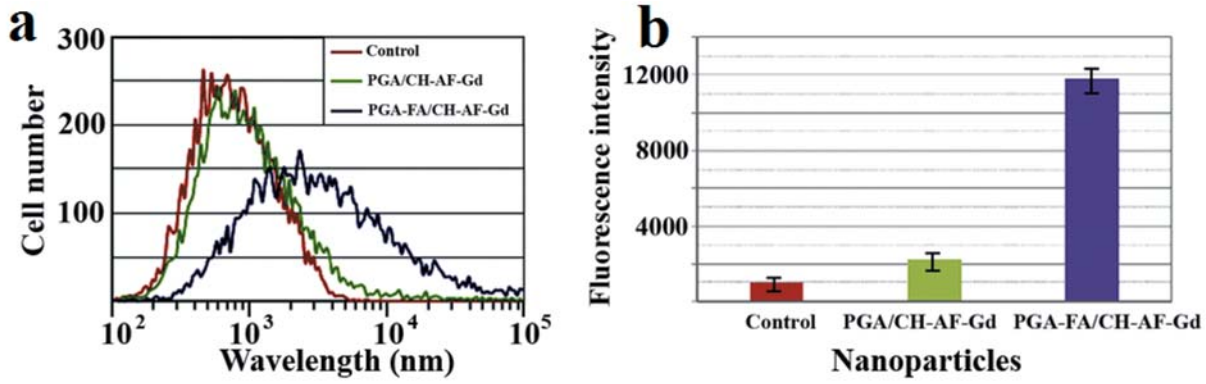

Figure 4. *FACS analysis of nanoparticle uptake. Folate-dependent uptake of nanoparticles was detected as described in the Methods. a) Fluorescence histograms of untreated HeDe cells (red), HeDe cells treated with folate-targeted γ-PGA-FA/CH-AF–Gd (blue) and non-folated γ-PGA/CH-AF–Gd nanoparticle (green). b) Mean fluorescence intensities of nanoparticles.*

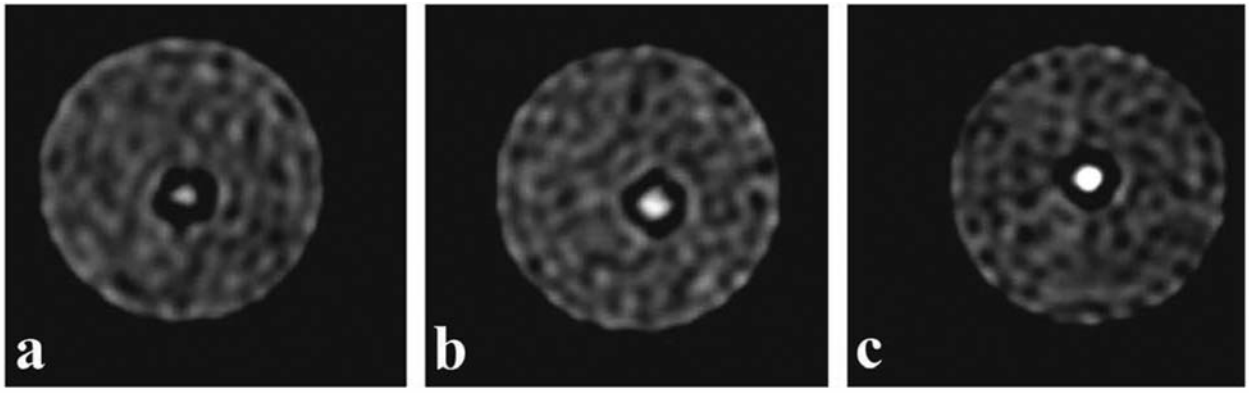

Figure 5. T_1-Weighted MR images of control HeDe cells (a), HeDe cell suspensions incubated with non-folated γ-PGA/CH-AF–Gd nanoparticles (b) and with folate-targeted γ-PGA-FA/CH-AF–Gd (c).

Fusion image slices of MRI and PET images (shown in Figure 7c) are useful in early tumor diagnosis as they combine the anatomic and metabolic information. PET part of the fusion image slices clearly exhibit the presence of the tumor, while the MRI part of picture provided its accurate localization.

Conclusion

This work describes the preparation, the *in vitro* and *in vivo* investigation of a novel, targeted, nanosized MRI contrast agents. Stable, folate-targeted nanoparticles as potential MRI contrast agents were obtained by the self-assembly of biopolymers containing paramagnetic gadolinium ions.

In vitro experiments confirmed that a significant proportion of these nanoparticles were internalized and selectively accumulated in targeted tumor cells that overexpress folate receptors. The results demonstrated that cellular uptake was folate receptor-dependent. Non-folated nanocarriers did not enter the cell membrane as their receptors could not recognize these particles.

The specificity of folate binding is expected to minimize the side-effects of folated nanoparticles. *In vivo* MRI contrast enhancement of folate-targeted nanoparticles was verified by using our F344 rat tumor model.

Fusion images were obtained by the combination of PET and MRI of tumor-bearing rats treated with folate-targeted nanoparticles visualizing simultaneously the anatomy and metabolism of the animal.

Our targeted nanoparticles are potential MRI contrast agents for diagnostic applications, and have the additional potential to be developed into delivery systems for therapeutic agents.

Acknowledgements

Financial support for this work was provided by the Hungarian National Development Agency (GOP-1.1.1-07/1-2008-0082),

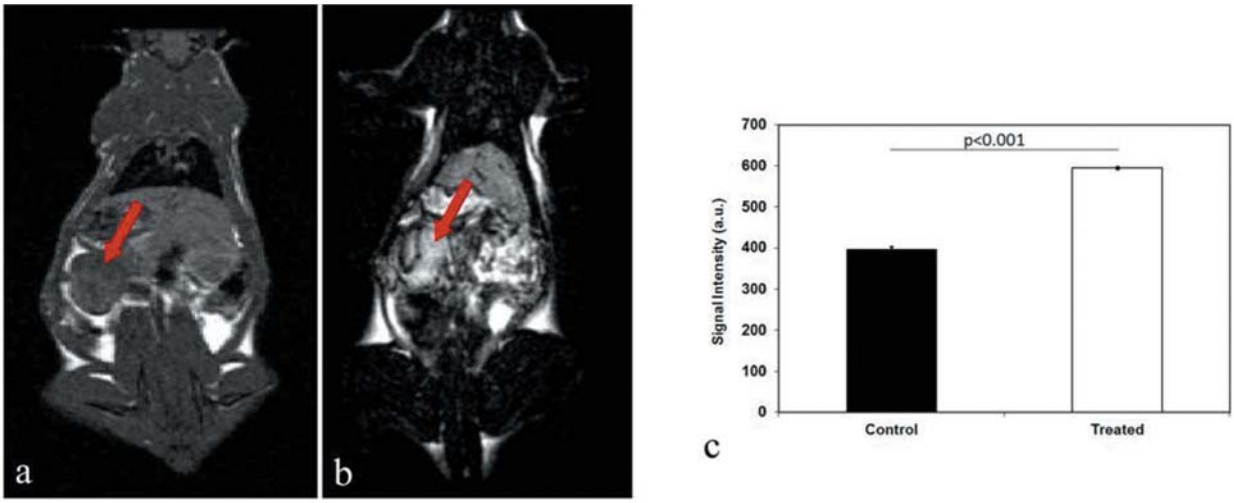

Figure 6. *Study on the uptake of γ-PGA-FA/CH-AF–Gd into HeDe tumors (a, b). The T1-weighted MRI (coronal slices) of Fischer 344 rats bearing HeDe tumors post-intravenous injection of 5% glucose solution as control (a) and γ-PGA-FA/CH-AF–Gd contrast agent (b). The increase in signal intensity of γ-PGA-FA/CH-AF–Gd can be visualized in treated HeDe tumors (b). Much less effect can be seen in the control tumor. (c) The graph also shows the significantly different signal intensity values between control and treated tumors.*

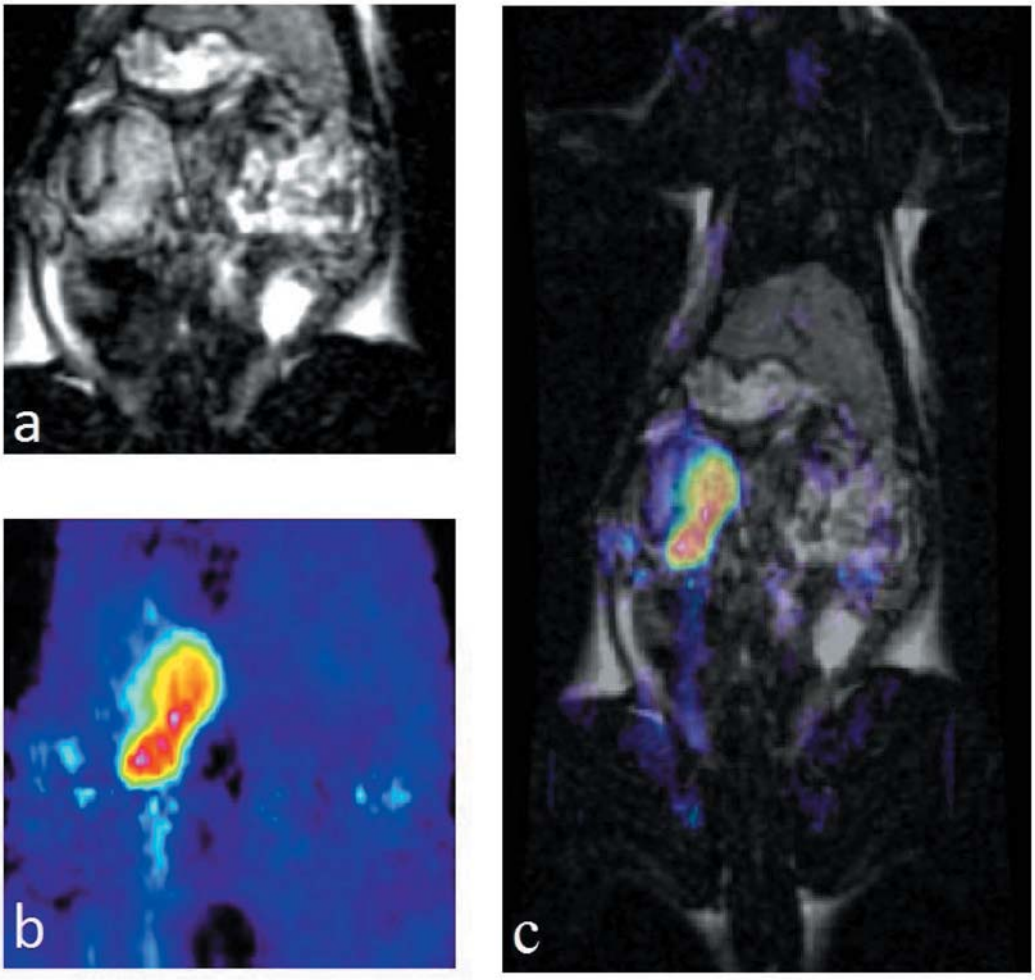

Figure 7. *Representative section of T1-weighted MR image (a) and PET image (b) and fusion image (c) of γ-PGA-FA/CH-AF–Gd-treated tumor-bearing rat. The fusion image combines the anatomic and metabolic information, which can facilitate early tumor diagnosis and accurate localization.*

Hungarian Scientific Research Fund (OTKA K77600), TÁMOP-4.2.1/B-09/1/KONV-2010-0007 This research was realized in the frames of TÁMOP 4.2.4. A/2-11-1-2012-0001 "National Excellence Program – Elaborating and operating an inland student and researcher personal support system". The project was subsidized by the European Union and co-financed by the European Social Fund. Authors thank Lajos Daróczi (Department of Solid State Physics, University of Debrecen, 4010 Debrecen, Hungary) for preparing SEM micrographs.

References

1 Dinauer N, Balthasar S, Weber C, Kreuter J, Langer K and von Briesen H: Selective targeting of antibody-conjugated nanoparticles to leukemic cells and primary T-lymphocytes. Biomaterials *26(29)*: 5898-5906, 2005.

2 Balthasar S, Michaelis K, Dinauer N, von Briesen H, Kreuter J and Langer K: Preparation and characterisation of antibody modified gelatin nanoparticles as drug carrier system for uptake in lymphocytes. Biomaterials *26(15)*: 2723-2732, 2005.

3 Zhang XX, Eden HS and Chen X: Peptides in cancer nanomedicine: drug carriers, targeting ligands and protease substrates. J Control Release *159(1)*: 2-13, 2012.

4 Herringson TP and Altin JG: Effective tumor targeting and enhanced anti-tumor effect of liposomes engrafted with peptides specific for tumor lymphatics and vasculature. Int J Pharm *411(1-2)*: 206-214, 2011.

5 Accardo A, Morisco A, Gianolio E, Tesauro D, Mangiapia G, Radulescu A, Brandt A and Morelli G: Nanoparticles containing octreotide peptides and gadolinium complexes for MRI applications. J Pept Sci *17(2)*: 154-162, 2011.

6 Daniels TR, Bernabeu E, Rodríguez JA, Patel S, Kozman M, Chiappetta DA, Holler E, Ljubimova JY, Helguera G and Penichet ML: The transferrin receptor and the targeted delivery of therapeutic agents against cancer. Biochim Biophys Acta *1820(3)*: 291-317, 2012.

7 Korkusuz H, Ulbrich K, Welzel K, Koeberle V, Watcharin W, Bahr U, Chernikov V, Knobloch T, Petersen S, Huebner F, Ackermann H, Gelperina S, Kromen W, Hammerstingl R, Haupenthal J, Gruenwald F, Fiehler J, Zeuzem S, Kreuter J, Vogl TJ and Piiper A: Transferrin-coated gadolinium nanoparticles as MRI contrast agent. Mol Imaging Biol *15(2)*: 148-154, 2013.

8 Holland JP, Evans MJ, Rice SL, Wongvipat J, Sawyers CL and Lewis JS: Annotating MYC status with ^{89}Zr-transferrin imaging. Nat Med *18(10)*: 1586-1591, 2012.

9 Mankoff DA, Link JM, Linden HM, Sundararajan L and Krohn KA: Tumor receptor imaging. J Nucl Med *49(2)*: 149S-163S, 2008.

10 Bunschoten A, Buckle T, Kuil J, Luker GD, Luker KE, Nieweg OE and van Leeuwen FW: Targeted non-covalent self-assembled nanoparticles based on human serum albumin. Biomaterials *33(3)*: 867-875, 2012.

11 Hwang do W, Ko HY, Lee JH, Kang H, Ryu SH, Song IC, Lee DS and Kim S: A nucleolin-targeted multimodal nanoparticle imaging probe for tracking cancer cells using an aptamer. J Nucl Med *51(1)*: 98-105, 2010.

12 Lim EK, Kim B, Choi Y, Ro Y, Cho EJ, Lee JH, Ryu SH, Suh JS, Haam S and Huh YM: Aptamer-conjugated magnetic nanoparticles enable efficient targeted detection of integrin αvβ3 *via* magnetic resonance imaging. J Biomed Mater Res A *102(1)*: 49-59, 2014.

13 Swanson SD, Kukowska-Latallo JF, Patri AK, Chen C, Ge S, Cao Z, Kotlyar A, East AT and Baker JR: Targeted gadolinium-loaded dendrimer nanoparticles for tumor-specific magnetic resonance contrast enhancement. Int J Nanomedicine *3(2)*: 201-210, 2008.

14 Yang HM, Park CW, Bae PK, Ahn T, Seo BK, Chung BH and Kim JD: Folate-conjugated cross-linked magnetic nanoparticles as potential magnetic resonance probes for *in vivo* cancer imaging. J Mater Chem B *1(24)*: 3035-3043, 2013.

15 Licciardi M, Giammona G, Du J, Armes SP, Tang Y and Lewis AL: New folate-functionalized biocompatible block copolymer micelles as potential anti-cancer drug delivery systems. Polymer *47(9)*: 2946-2955, 2006.

16 Weitman SD, Lark RH, Coney LR, Fort DW, Frasca V, Zurawski VR Jr. and Kamen BA: Distribution of the folate receptor GP38 in normal and malignant cell lines and tissues. Cancer Res *52(12)*: 3396-3401, 1992.

17 Prabaharan M, Grailer JJ, Pilla S, Steeber DA and Gong S: Folate-conjugated amphiphilic hyperbranched block copolymers based on Boltorn® H40, poly(L-lactide) and poly(ethylene glycol) for tumor-targeted drug delivery. Biomaterials *30(16)*: 3009-3019, 2009.

18 Tyagi N and Ghosh PC: Folate receptor mediated targeted delivery of ricin entrapped into sterically stabilized liposomes to human epidermoid carcinoma (KB) cells: effect of monensin intercalated into folate-tagged liposomes. Eur J Pharm Sci *43(4)*: 343-353, 2011.

19 Zhang W, Shi Y, Chen Y, Ye J, Sha X and Fang X: Multifunctional Pluronic P123/F127 mixed polymeric micelles loaded with paclitaxel for the treatment of multidrug resistant tumors. Biomaterials *32(11)*: 2894-2906, 2011.

20 Zhu H, Liu F, Guo J, Xue J, Qian Z and Gu Y: Folate-modified chitosan micelles with enhanced tumor targeting evaluated by near infrared imaging system. Carbohydr Polym *86(3)*: 1118-1129, 2011.

21 Chandrasekar D, Sistla R, Ahmad FJ, Khar RK and Diwan PV: The development of folate-PAMAM dendrimer conjugates for targeted delivery of anti-arthritic drugs and their pharmacokinetics and biodistribution in arthritic rats. Biomaterials *28(3)*: 504-512, 2007.

22 Kukowska-Latallo JF, Candido KA, Cao Z, Nigavekar SS, Majoros IJ, Thomas TP, Balogh LP, Khan MK and Baker JR Jr.: Nanoparticle targeting of anticancer drug improves therapeutic response in animal model of human epithelial cancer. Cancer Res *65(12)*: 5317-5324, 2005.

23 Gabizon A, Horowitz AT, Goren D, Tzemach D, Shmeeda H and Zalipsky S: *In vivo* fate of folate-targeted polyethylene-glycol liposomes in tumor-bearing mice. Clin Cancer Res *9(17)*: 6551-6559, 2003.

24 Li H, Piao L, Yu B, Yung BC, Zhang W, Wang PG, Lee JL and Lee RJ: Delivery of calf thymus DNA to tumor by folate receptor targeted cationic liposomes. Biomaterials *32(27)*: 6614-6620, 2011.

25 Tsai SW, Liaw JW, Hsu FY, Chen YY, Lyu MJ and Yeh MH: Surface-modified gold nanoparticles with folic acid as optical probes for cellular imaging. Sensors *8*: 6660-6673, 2008.

26 Lin JJ, Chen JS, Huang SJ, Ko JH, Wang YM, Chen TL and Wang LF: Folic acid–Pluronic F127 magnetic nanoparticle clusters for combined targeting, diagnosis, and therapy applications. Biomaterials *30(28)*: 5114-5124, 2009.

27 Hou Z, Zhan C, Jiang Q, Hu Q, Li L, Chang D, Yang X, Wang Y, Li Y, Ye S, Xie L, Yi Y and Zhang Q: Both FA- and mPEG-conjugated chitosan nanoparticles for targeted cellular uptake and enhanced tumor tissue distribution. Nanoscale Res Lett *6(1)*: 563, 2011.
28 Werner ME, Karve S, Sukumar R, Cummings ND, Copp JA, Chen RC, Zhang T and Wang AZ: Folate-targeted nanoparticle delivery of chemo- and radiotherapeutics for the treatment of ovarian cancer peritoneal metastasis. Biomaterials *32(33)*: 8548-8554, 2011.
29 Weissleder R: Molecular imaging in cancer. Science *312(5777)*: 1168-1171, 2006.
30 Antoch G and Bockisch A: Combined PET/MRI: a new dimension in whole-body oncology imaging? Eur J Nucl Med Mol Imaging *36(1)*: S113-S120, 2009.
31 Patel D, Kell A, Simard B, Xiang B, Lin HY and Tian G: The cell labeling efficacy, cytotoxicity and relaxivity of copper-activated MRI/PET imaging contrast agents. Biomaterials *32(4)*: 1167-1176, 2011.
32 Jugendhofer MS, Wehrl HF, Newport DF, Catana C, Siegel SB, Becker M, Thielscher A, Kneilling M, Lichy MP, Eichner M, Klingel K, Reischl G, Widmaier S, Röcken M, Nutt RE, Machulla HJ, Uludag K, Cherry SR, Claussen CD and Pichler BJ: Simultaneous PET-MRI: a new approach for functional and morphological imaging. Nat Med *14(4)*: 459-65, 2008.
33 Pichler BJ, Kolb A, Nägele T and Schlemmer HP: PET/MRI: paving the way for the next generation of clinical multimodality imaging applications. J Nucl Med *51(3)*: 333-336, 2010.
34 Kim SM, Chae MK, Yim MS, Jeong IH, Cho J, Lee C and Ryu EK: Hybrid PET/MR imaging of tumors using an oleanolic acid-conjugated nanoparticle. Biomaterials *34(33)*: 8114-8121, 2013.
35 Hajdu I, Bodnár M, Filipcsei G, Hartmann JF, Daróczi L, Zrínyi M and Borbély J: Nanoparticles prepared by self-assembly of chitosan and poly-γ-glutamic acid. Colloid Polym Sci *286(3)*: 343–350, 2008.
36 Keresztessy Z, Bodnár M, Ber E, Hajdu I, Zhang M, Hartmann JF, Minko T and Borbély J: Self-assembling chitosan/poly-γ-glutamic acid nanoparticles for targeted drug delivery. Colloid Polym Sci *287(7)*: 759-765, 2009.
37 HMG CoA reductase inhibitor fluvastatin arrests the development of implanted hepatocarcinoma in rats. Anticancer Res 23(5A): 3949-3854, 2003.
38 Trencsényi G, Kertai P, Somogyi C, Nagy G, Dombradi Z, Gacsi M and Banfalvi G: Chemically induced carcinogenesis affecting chromatin structure in rat hepatocarcinoma cells. DNA Cell Biol *26(9)*: 649-655, 2007.
39 Workman P, Twentyman P, Balkwill F, Balmain A, Chaplin D, Double J, Embleton J, Newell D, Raymond R, Stables J, Stephens T and Wallace J: United Kingdom Co-ordinated Committee on Cancer Research (UKCCCR) Guidelines for the welfare of animals in experimental neoplasia (second edition). Br J Cancer *77(1)*: 1-10, 1998.
40 Trencsenyi G, Kertai P, Bako F, Hunyadi J, Marian T, Hargitai Z, Pocsi I, Muranyi E, Hornyak L and Banfalvi G: Renal capsule-parathymic lymph node complex: a new *in vivo* metastatic model in rats. Anticancer Res *29(6)*: 2121-2126, 2009.

Received November 12, 2013
Revised December 5, 2013
Accepted December 6, 2013